ACTA METALLURGICA SLOVACA
2021, VOL. 27, NO. 4, 203-206

RESEARCH PAPER

PREPARATION OF TRANSPARENT $MgAl_2O_4$ CERAMICS BY PULSED ELECTRIC CURRENT SINTERING USING TWO-STEP HEATING METHOD

Yen Ngoc Nguyen[1)†], Hai Minh Le[1,2)†], Tu Anh Dao[1)], Hung Ngoc Tran[3)], Tue Ngoc Nguyen[3)], Thang Hong Le[1)], Khanh Quoc Dang[1)]*

[1] School of Materials Science and Engineering, Hanoi University of Science and Technology, No.1 Dai Co Viet, Hai Ba Trung, Hanoi 10000, Vietnam
[2] Viettel Aerospace Institute, Viettel Group, Lot D26, Cau Giay New Urban Area, Yen Hoa, Cau Giay, Hanoi, 10000, Vietnam
[3] School of Chemical Engineering, Hanoi University of Science and Technology, No1, Dai Co Viet, Hai Ba Trung, Hanoi 10000, Vietnam

*Corresponding author: khanh.dangquoc@hust.edu.vn, tel.: +84 24 3868 0355, School of Materials Science and Engineering, Hanoi University of Science and Technology, 10000, Hanoi, Vietnam
†These authors made equal contributions

Received: 02.10.2021
Accepted: 23.11.2021

ABSTRACT

Transparent $MgAl_2O_4$ ceramics were fabricated by pulsed electric current sintering (PECS) employing a two-step sintering mode. First, nanoscale $MgAl_2O_4$ powders were produced by solution combustion synthesis from hydrated nitrate compounds and urea. Subsequently, the synthesized powders were sintered by PECS with a heating rate of 100°C/min under an applied pressure of 100 MPa. The sintering process was conducted according to a two-step heating profile. At the first step, the temperature increased to 1050, 1100, and 1150°C, followed by a dwell time of 60 min. The second-step sintering was carried out at 1300, 1350, and 1400°C for 20 min. The transparent ceramics sintered at 1050°C / 60 min – 1400°C / 20 min exhibited transmittance over 80% in infrared range. In addition, transparent samples presented a Vickers hardness up to 30 GPa for sintering mode of 1150°C / 60 min – 1400°C / 20 min.

Keywords: transparent ceramics; $MgAl_2O_4$; PECS; two-step sintering

INTRODUCTION

Recently, transparent ceramics have received increasing attention from scientists owing to transmittance in a wide range of wavelengths, excellent mechanical properties, and resistance at high temperature [1-7]. Magnesium aluminate $MgAl_2O_4$ spinel is one of the most commonly-used transparent ceramics as it presents an isotropic crystal structure, which curbs diffuse transmission when the light passes through the material. In addition, this material allows light with wavelengths from the ultraviolet to the mid-infrared region to transmit through it [8].
Production of transparent ceramics must concurrently meet two strict requirements including high purity (up to 99.5%) and nearly full density (>99%) to prevent the light scattering caused by impurities and pores. Meanwhile, thanks to the isotropic crystal lattice of the material, no limitation of grain size is required for transparent $MgAl_2O_4$ ceramics. Moreover, the increase in grain size leads to the decrease in light diffuse transmission at the grain boundary, thereby improving the material transmittance [8]. Nevertheless, the mechanical strength of materials is weakened with the increase in grain size according to the Hall-Petch relation. Therefore, a compromise between improvement in transmittance and enhancement to mechanical strength is essential to achieve high-quality transparent ceramics.
Production of transparent $MgAl_2O_4$ ceramics involves two main stages, powder synthesis and densification. For the powder synthesis, the synthesized powders must contain solely one single phase to minimize light scattering, and nanoparticles to promote the consolidation process in the next sintering step [9, 10]. Recently, chemical synthesis methods are considered as an effective bottom-up approach to prepare nanostructured materials with high purity and uniform particle size. $MgAl_2O_4$ nanoparticles have been synthesized by chemical methods comprising sol-gel [11], hydrothermal synthesis [12], and chemical precipitation [13]. Solution Combustion Synthesis (SCS) is a chemical precipitation method whereby a reaction occurs due to self-propagating heat using a mixture of oxidizers and fuels. In the case of ultrafine $MgAl_2O_4$ powder, the oxidizers including hydrated nitrate compounds $Mg(NO_3)_2.6H_2O$ and $Al(NO_3)_3.9H_2O$ were integrated with fuels such as urea, glycine, and alanine [14].
Regarding material consolidation, pulsed electric current sintering (PECS) is well-known as a superior method to fabricate high-quality transparent ceramics [15, 16]. $MgAl_2O_4$ transparent ceramics were prepared by PECS at 1300°C with a slow heating rate smaller than 10°C /min [17, 18]. Meanwhile, Suarez et.al. reported that $MgAl_2O_4$ transparent ceramics were produced at a high temperature of 1550°C with a high heating rate of 100°C /min [19]. In addition to the conventional single-step sintering process, a two-step heating method accompanied by PECS has been selected to produce transparent ceramics [20]. In a two-step heating profile, the first step is implemented at a low temperature, and subsequently, the temperature increases to the sintering temperature to densify the bulk

materials. By virtue of the two-step heating method, bulk samples yield nearly full relative density with uniform fine particle size after sintering at a low temperature with a high heating rate [20].

Previous reports stated the synthesis of transparent $MgAl_2O_4$ ceramics. Specifically, $MgAl_2O_4$ nanopowder was synthesized by SCS method using a mixture of $Mg(NO_3)_2.6H_2O$ and $Al(NO_3)_3.9H_2O$ as oxidizers, and urea as a fuel. The synthesized powder contained a large agglomeration of nanoparticles. To disaggregate nanoparticles, low energy ball milling with various milling times and ball/powder ratios was investigated to optimize the milling efficiency [21]. The transparent $MgAl_2O_4$ ceramics were successfully fabricated by PECS accompanied by a two-step heating profile [22]. In this study, the sintering process of transparent $MgAl_2O_4$ ceramic was optimized by varying the sintering temperature at both the first and second steps.

MATERIAL AND METHODS

The starting materials were aluminium nitrate hydrated ($Al(NO_3)_3.9H_2O$) (99.997%, Sigma Aldrich, Germany) and magnesium nitrate hydrated ($Mg(NO_3)_2.6H_2O$) (99.999%, Sigma Aldrich, Germany) as oxidizers and urea (CH_4N_2O) (99.5%, Sigma Aldrich, Germany) as fuel. The precursor mixture was stoichiometrically balanced with a molar ratio of 3:6:20, and dissolved in distilled water. Subsequently, the aqueous solution was placed in an electric resistance furnace (Linn HT1300, Germany), which was preheated at 500°C. The combustion reaction occurred according to the following reaction to form a voluminous product.

$$3Mg(NO_3)_2\,(aq) + 6Al(NO_3)_3\,(aq) + 20CH_4N_2O\,(aq) \rightarrow 3MgAl_2O_4(s) + 20CO_2(g) + 40H_2O(g) + 32N_2(g)$$

The synthesized product was calcined at 1100°C for 2 h. After the calcination, the powder was milled for 48 h in an ethanol solvent using alumina balls with a ball – powder mass ratio of 20/1. Using graphite die with an inner diameter of 10 mm, the powder was sintered by an SPS machine (LABOX 1550i75S, Japan) under a high vacuum (< 5 x 10^{-3} Pa) with an applied uniaxial pressure of 100 MPa. Sintering process was conducted with 100°C/min heating rate using two-step sintering profile, namely 1050, 1100, and 1150°C for 60 min followed by 1300, 1350, and 1400°C for 20 min. After sintering, samples were polished by a slurry of Al_2O_3 powder with a particle size of 0.05 μm for 80 h.

The microstructure of bulk samples was characterized using the field emission scanning electron microscopy (FE-SEM, Hitachi S4800, Singapore). Using SEM images, grain size and size distribution were determined 100 times by ImageJ software. Ultraviolet-visible (UV-Vis) and Fourier transform infrared (FTIR) spectroscopies were applied to determine the transmission spectra of samples from the ultraviolet range to the infrared range (190-8000 nm). The obtained transmittance was converted into the transmittance of samples with a thickness of 1 mm as follows:

$$\tau_o = \tau_x^{1/x} \tag{1.}$$

where τ_o and τ_x are the transmittance of samples with a 1-mm and x-mm thickness, respectively. Vickers hardness was obtained by dividing the load by the square area of indentation as follows:

$$H_V = 1{,}8544.10^{-3}\frac{F}{d^2} \tag{2.}$$

where HV is Vickers hardness, F denotes the load, and d signifies the average of two indentation diagonals. Additionally, fracture toughness K_{IC} could be determined by Vickers hardness testing as follows [23]:

$$K_{IC} = 0.016 \times \left(\frac{c}{d}\right)^{-3/2} \times H_v \times d^{1/2} \tag{3.}$$

where c represents the length of cracks.

RESULTS AND DISCUSSION

The morphology of the $MgAl_2O_4$ sample sintered via a two-step sintering mode of 1100°C/60 min – 1400°C/20 min was observed by SEM and shown in **Fig. 1**. Most of the grains presented submicron size and were well dispersed without any local size growth. The grain size distribution of sintered samples was in a narrow range from 50 to 300 nm, and most of the grain size was within the 150-200 nm range. The mean grain size of samples which were sintered at 1100°C /60 min – 1400°C/20 min was approximately 177 nm.

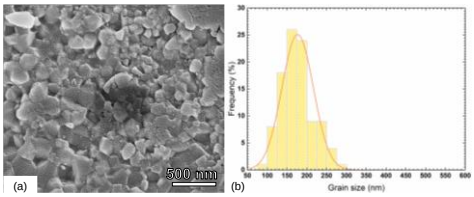

Fig. 1 (a) SEM image and (b) grain size distribution of $MgAl_2O_4$ sample sintered via two-step sintering mode of 1100°C/60 min – 1400°C/20 min

Fig. 2 Photograph of transparent $MgAl_2O_4$ ceramic samples sintered via different two-step sintering modes

The presence of $MgAl_2O_4$ samples produced by PECS via different sintering modes of first–step temperatures (1050, 1100, and 1150°C), and second–step temperatures (1300, 1350, and 1400°C) is displayed in **Fig. 2**. The $MgAl_2O_4$ samples were virtually translucent at the second–step temperatures of 1300°C and 1350°C, while samples that were sintered at the second–step temperature of 1400°C became transparent regardless of first-step sintering temperature. The results suggested that the second-step sintering temperature had a significant influence on the transmission of materials rather than the first-step temperature. When the second-step temperature was fixed at 1400°C for 20 min, all the samples with various first-step temperatures showed good transparency, which could be recognized with the naked eye.

Fig. 3 shows the transmission spectrum of $MgAl_2O_4$ samples sintered at the different first-step temperatures and the second-step temperatures of 1400°C in ultraviolet-visible range (280 – 1000 nm) and infrared range (3500 – 8000 nm) with 1 mm thickness as shown in Eq.1. Results reveal that samples had poor transmittance in the ultraviolet range. At visible wavelength, transmittance linearly increased, and subsequently reached a maximum value up to 80% in the infrared range, which is close to theoretical maximum transmittance (87%) [2]. Furthermore, the transmittance at the wavelengths of 550nm (T_{550}) and 4000 nm (T_{4000}) was changed with the variation in the first–step sintering temperature. To be specific, T_{550} was approximately 28% for the first-step temperature of 1050°C, 35% for 1150°C and 40% for 1100°C. At 4000 nm wavelength, T_{4000} was approximately 62%, 77%, and 80% corresponding to the first–step temperatures of 1100°C,

1150°C, and 1050°C. **Fig. 4** represents the measured Vickers hardness of transparent MgAl2O4 samples sintered at different first–step temperatures (1050, 1100, and 1150°C) and the second–step temperature of 1400°C with a load of 20N.

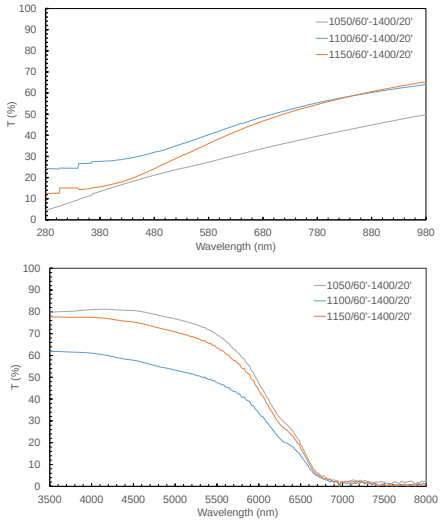

Fig. 3 Transmission spectra of transparent $MgAl_2O_4$ ceramic samples in the ultraviolet-visible range (280 – 1000 nm) and infrared range (3500 – 8000 nm)

The Vickers hardness increased along with an increasing the first–step temperature. The average hardness values were 14.21, 19.86, 29.32 GPa for the first step sintering temperatures of 1050, 1100, and 1150°C, respectively. The maximum value of 29.32 GPa was attained via a two-step sintering mode of 1150°C/ 60 min – 1400°C/ 20 min. Using impression diagonals obtained by Vickers hardness, fracture toughness K_{IC} of $MgAl_2O_4$ samples was calculated via Eq.3 and represented in **Fig. 5**. The value of fracture toughness increased as the Vickers hardness increased. Specifically, the lowest value of 1.09 MPa.m$^{1/2}$ corresponds to sample sintered at 1050°C/ 60 min – 1400°C/ 20 min. At the first step temperature of 1100°C, the fracture toughness amounted to 1.18 MPa.m$^{1/2}$. The maximum value was approximately 2.12 MPa.m$^{1/2}$, achieved by samples sintered at 1150°C/ 60 min – 1400°C/ 20 min.

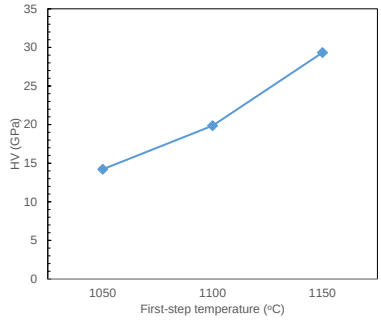

Fig. 4 Vickers Hardness of transparent $MgAl_2O_4$ samples sintered at different first–step temperatures (1050, 1100, and 1150°C) and the second–step temperature of 1400°C with a load of 20N

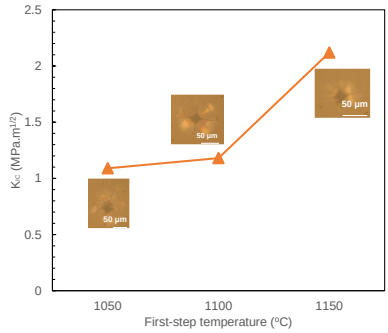

Fig. 5 Fracture toughness (K_{IC}) of transparent $MgAl_2O_4$ samples sintered at different first–step temperatures (1050, 1100, and 1150°C) and the second–step temperature of 1400°C

Table 1 Recent research on transparent $MgAl_2O_4$ ceramics prepared by PECS

Reference	Initial powder: Synthesis method	Initial powder: Particle size (nm)	Sintering parameters: Temperature/ Time/ Pressure/ Heating rate	Post-sintering treatment	Grain size	Hardness (GPa)	Fracture toughness (MPa.m$^{1/2}$)	Transmittance (%): T_{300}	T_{550}	T_{4000}	T_{5500}
Pourshamsi et. al., 2019 [24]	Commercial powder	80-220	1400°C/ 15 min/ 80 MPa/ 15°C/min	Annealing at 1200°C for 5h	~10µm	n/a	n/a	n/a	24	75	53
Necina et.al., 2020 [25]	Commercial powder	n/a	1200°C for 30 min and 1500°C for 60 min/ 80 MPa/ 100°C/min up to 800°C and 25°C/min up to 1500°C	n/a	980 nm	n/a	n/a	45.3	68	n/a	n/a
Nassaj-pour-Esfahani et. al., 2020 [26]	Commercial powder	250	1550°C/ 20 min/ 85 MPa/ n/a	n/a	n/a	7.7	5.1	<10	30	82	63
This work	Solution combustion synthesis	27	1050, 1100, 1150°C for 60 min and 1400°C for 20 min/ 100 MPa/ 100°C/min	Not required	177 nm	14.21/ 19.86/ 29.32	1.09/ 1.18/ 2.12	6.04/ 24.1/ 12.6	25.44 / 37.56 / 32.5	81.01/ 61.03/ 77.46	69.46/ 47.48/ 63.42

To verify the effect of the two-step sintering method on the product quality, the results attained by the two-step sintering process were compared to ones achieved by PECS in recent research over the last 3 years (Table 1). The two-step sintering method in this work could, concurrently, reduce the sintering temperature and increase the heating rate without deterioration in product quality as compared to the other studies. Owing to the fine synthesized powder, mechanical characteristics including Vickers hardness and fracture toughness were remarkably enhanced, while the transmittance of $MgAl_2O_4$ samples could maintain the appropriate values. This suggests the feasibility of PECS accompanied with a two-step sintering method to produce high-quality transparent ceramic from combustion-synthesized nanopowders.

CONCLUSION

Transparent $MgAl_2O_4$ ceramics were fabricated by PECS using the two-step sintering method. To investigate the influence of temperature on the optical and mechanical properties of materials, the first-step and second-step temperatures were varied from 1050°C to 1150°C, and from 1300°C to 1400°C, respectively. The microstructure of sintered samples presented submicron grain size with narrow size distribution. $MgAl_2O_4$ samples sintered at the second-step temperature of 1400°C exhibited transparency under the observation. Meanwhile, the transmittance of $MgAl_2O_4$ ceramics could reach up to 50% in the visible range for 1100°C /60 min – 1400°C /20 min and up to 80% in the infrared range for 1050°C /60 min – 1400°C /20 min. In addition, samples sintered at sintering mode of 1150°C/60 min – 1400°C /20 min exhibited excellent mechanical properties, namely Vickers micro-hardness of 29.32 GPa and fracture toughness of 2.12 $MPa.m^{1/2}$.

Acknowledgement: This work was funded by the Vietnam Ministry of Education and Training [grant number B2018-BKA-63]. The authors are grateful for the support of Nanko Laboratory, Nagaoka University of Technology, Japan for performing the sintering process experiments.

REFERENCES

1. S.F.Wang et al.: Progress in Solid State Chemistry, 41(1-2), 2013, 20-54. https://doi.org/10.1016/j.progsolidstchem.2012.12.002.
2. R. Bidulsky, M.A. Grande, L. Ferraris, P. Ferraris, J. Bidulska: Acta Polonica Physica A, 118(5), 2010, 802-803. https://doi.org/10.12693/APhysPolA.118.802.
3. E. Fracchia, F.S. Gobber, M. Rosso, M.A. Grande, J. Bidulska, R. Bidulsky: Materials, 12(21), 2019, 3475. http://doi.org/10.3390/ma12213475.
4. A. Goldstein, A. Krell: Journal of the American Ceramic Society, 99(10), 2016, 3173-3197. https://doi.org/10.1111/jace.14553
5. H. Shahbazi, M. Tataei, M. H. Enayati, A. Shafeiey, M. A. Malekabadi: Journal of Alloys and Compounds, 785, 2019, 260-285. https://doi.org/10.1016/j.jallcom.2019.01.124
6. Z. Shi, Q. Zhao, B. Guo, T. Ji, H. Wang: Materials & Design, 193(June), 2020, 108858. https://doi.org/10.1016/j.matdes.2020.108858.
7. A. Zegadi, M. Kolli, M. Hamidouche, G. Fantozzi: Ceramics International, 44(15), 2018, 18828-18835. https://doi.org/10.1016/j.ceramint.2018.07.117.
8. M. R. Merac, H. J. Kleebe, M. M. Müller, I. E. Reimanis: Journal of the American Ceramic Society, 96(11), 2013, 3341–3365. https://doi.org/10.1111/jace.12637.
9. L. Zych, R. Lach, A. Wajler: Ceramics International, 40(7), 2014, 9783-9790. https://doi.org/10.1016/j.ceramint.2014.02.066.
10. S. Nam, M. Lee, B. Kim, Y. Lee, S. Kang: Ceramics International, 43(17), 15352-15359. http://doi.org/10.1016/j.ceramint.2017.08.075.
11. S. Sanjabi, A. Obeydavi: Journal of Alloys and Compounds, 645(5), 2015, 535–540. https://doi.org/10.1016/j.jallcom.2015.05.107.
12. J. Duan et al.: IOP Conference Series: Earth and Environmental Science, 81, 2017, 012-028. https://doi.org/10.1088/1755-1315/81/1/012028.
13. H. Li, Y. Q. Liu, H. Liu, Z. J. Yang: Materials Research Innovations, 19(9), 2015, S9-20-S9-23. https://doi.org/10.1179/1432891715Z.0000000001910.
14. R. Ianoș, I. Lazău, C. Păcurariu, P. Barvinschi: Materials Research Bulletin, 43(12), 2008, 3408-3415. https://doi.org/10.1016/j.materresbull.2008.02.003.
15. A. Talimian, V. Pouchly, H. F. El-Maghraby, K. Maca, D. Galusek: Journal of the European Ceramic Society, 40(6), 2020, 2417-2425. https://doi.org/10.1016/j.jeurceramsoc.2020.02.012.
16. V. Nečina, W. Pabst: Journal of the European Ceramic Society, 40(15), 2020, 6043-6052. https://doi.org/10.1016/j.jeurceramsoc.2020.06.056.
17. K. Morita, B. N. Kim, K. Hiraga, H. Yoshida: Scripta Materialia, 58(12), 2008, 1114-1117. https://doi.org/10.1016/j.scriptamat.2008.02.008.
18. G. Bonnefont, G. Fantozzi, S. Trombert, L. Bonneau: Ceramics International, 38(1), 2012, 131-140. http://dx.doi.org/10.1016/j.ceramint.2011.06.045.
19. M. Suarez, V. Rocha, A. Fernandez, J. L. Menendez, R. Torrecillas: Ceramics International, 40(3), 2014, 4065-4069. https://doi.org/10.1016/j.ceramint.2013.08.060.
20. M. Nanko, Q.K. Dang: Advances in Applied Ceramics, 113(2), 2014, 80-84. https://doi.org/10.1179/1743676113Y.0000000109.
21. N. N Yen, C. H. D. Anh, B. T. N. Mai, D. Q. Khanh, L. M. Hai: Journal of Science and Technology-Technical Universities, 129, 2018, 047-053.
22. N. N. Yen, D. A. Tu, L. M. Hai, D. Q. Khanh, M. Nanko: Acta Metallurgica Slovaca, 25(3), 2019, 186-192. https://doi.org/10.12776/AMS.V25I3.1313.
23. A.G. Evans, E.A. Charles: Journal of the American Ceramic Society, 59 (7-8), 1976, 371-372. https://doi.org/10.1111/J.1151-2916.1976.TB10991.X.
24. A. Pourshamsi, A. Alhaji, R. Emadi: Ceramics International, 45(6), 2019, 7151-7156. https://doi.org/10.1016/j.ceramint.2018.12.221.
25. V. Nečina, W. Pabst: Journal of the European Ceramic Society, 40(15), 2020, 6043-6052. https://doi.org/10.1016/j.jeurceramsoc.2020.06.056.
26. A. H. Nassajpour-Esfahani, R. Emadi, A. Alhaji, A. Bahrami, M. R. Haftbaradaran-Esfahani: Journal of Alloys and Compounds, 830, 2020, 154588. https://doi.org/10.1016/j.jallcom.2020.154588.